On the Deployment of Heterogeneous Sensor Networks for Detection of Mobile Targets

Loukas Lazos and Radha Poovendran
Network Security Laboratory (NSL)
University of Washington, Seattle, WA
llazos, rp3@u.washington.edu

James A. Ritcey
Department of Electrical Engineering,
University of Washington, Seattle, WA
ritcey@ee.washington.edu

***Abstract*— Detecting targets moving inside a field of interest is one of the fundamental services of Wireless Sensor Networks. The network performance with respect to target detection, is directly related to the placement of the sensors within the field of interest. In this paper, we address the problem of wireless sensor deployment, for the purpose of detecting mobile targets. We map the target detection problem to a line-set intersection problem and derive analytic expressions for the probability of detecting mobile targets. Compared to previous works, our mapping allows us to consider sensors with heterogeneous sensing capabilities, thus analyzing sensor networks that employ multiple sensing modalities. We show that the complexity of evaluating the target detection probability grows exponentially with the network size and, hence, derive appropriate lower and upper bounds. We also show that maximizing the lower bound is analogous to the problem of minimizing the average symbol error probability in 2-dimensional digital modulation schemes over Additive White Gaussian Noise, that is, in turn, addressed using the circle packing problem. Using this analogy, we derive sensor constellations from well known signal constellations with low average symbol error probability.**

I. Introduction

One of the prominent applications of Wireless Sensor Networks (WSN) is to detect targets crossing a Field of Interest (FoI). As an example, in a physical intrusion detection system, sensors are deployed to detect objects moving within the FoI. In cases where the FoI is easily accessible, deploying the sensors in a deterministic manner provides worst case guarantees on the WSN performance, that are not achievable by a stochastic deployment.

The quality of target detection achieved by a WSN can be quantified by evaluating the probability of detecting a target by at least one sensor [4]. Evaluating the detection probability by at least one sensor provides a worst case guarantee for the detection performance of the WSN. In this paper, we analyze the following target detection problem. Given a planar FoI and N sensors, *determine the WSN constellation that yields the maximum target detection probability.*

The target detection probability is a function of the number of sensors deployed, the relative positions of the sensors (WSN constellation), as well as the modalities used to detect targets. The sensing modality defines the size and shape of the sensing area of each sensor. Oftentimes, a multimodal approach is preferred to increase the robustness of target detection, by deploying sensors of different sensing modalities, such as acoustic, seismic, optical, or infrared. In such a case, the sensor devices have heterogeneous sensing areas of arbitrary shape. This reality is significantly different from the unit disk model assumed in previous works [1], [4], [5], [10], or the assumption of identical sensing areas [1], [4]–[6], [8], [10], [14].

A. Our Contributions

We map the target detection problem to a line-set intersection problem. Using tools from Integral Geometry we derive analytical formulas that characterize the target detection probability when sensors are deterministically deployed. Compared to previous works [1], [4]–[6], [8], [10], [11], [14], we evaluate the target detection capability for WSN with devices of heterogeneous sensing capabilities. Based on our mapping, we show the number of terms in the analytical expression of the probability of target detection grows exponentially with the network size. We therefore provide appropriate lower and upper bounds.

We show that as the pairwise distance among the sensors increases, the lower bound asymptotically approaches the upper bound and, hence, the probability of target detection increases. We also show that maximizing the lower bound in the target detection problem is analogous to minimizing the average symbol error probability in 2-dimensional digital modulation schemes over an Additive White Gaussian Noise (AWGN) channel. In turn, the latter problem can be addressed by considering the circle packing problem. Inspired by this analogy, we examine the performance of known signal constellations on the target detection problem.

B. Paper Organization

The rest of the paper is organized as follows. In Section II, we present related work. In Section III, we state our model assumptions and map the target detection problem to a line-set intersection problem. In Section IV, we derive exact analytical formulas for the target detection probability. In Section V, we describe the analogy of target detection to the 2-dimensional digital modulation schemes, over an AWGN channel. In Section VI, we present our performance evaluation and in Section VII, we present our conclusions.

II. Related Work

The problem of detecting mobile targets in WSN has been a topic of extensive study under different metrics and assumptions [1], [4]–[6], [8], [10], [11], [14], [17]. In [10],

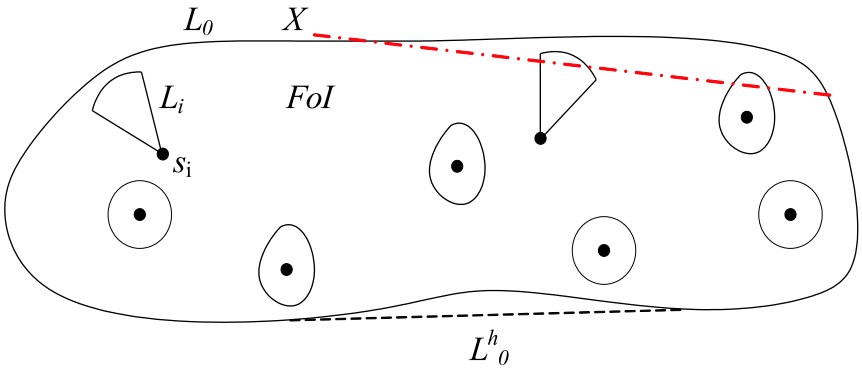

Fig. 1. A wireless sensor network monitoring an FoI with perimeter length L_0 and convex hull perimeter L_0^h. The target X is crossing the FoI moving on a straight line. The sensors deployed have heterogeneous sensing areas of different shape.

the authors investigate the tradeoff between the target detection quality and power conservation. They assume that nodes are randomly deployed within a planar FoI, and have sensing areas that follow the unit disk model. Given a target X moving on a straight line, they derive the mean time until X is first detected. They also provide sleeping pattern algorithms that lead to power conservation, while guaranteeing a minimum response time to detecting a target crossing the FoI.

In [4], the authors provide analytic formulas for the mean delay until a target is detected, when targets move on a straight line at a constant speed. The authors consider a system model where N sensors are randomly distributed within an FoI, with each sensor having identical sensing areas that follow the unit disk model. In their derivations, they also take into account the sleeping pattern of the sensors.

In [14], the authors propose a collaborative detection model, where sensors collectively arrive at a consensus about the presence of a target. While the problem addressed in [14] is the coverage of the FoI, the problem formulation can be indirectly used to also evaluate the target detection probability. It is assumed that the detection capability of each sensor decays as a function of distance and hence, the sensing area of each sensor follows the unit disk model. In terms of performance metrics, the authors consider the minimum exposure path, that is, the path for which the target is least exposed to detection, and the maximum exposure path, that is, the path for which the target is most exposed to detection.

In [6], the authors consider the same collaborative detection model as in [14], with sensors collectively determining the presence of a target. Sensors are assumed to be randomly deployed within the FoI and the sensing capability of each sensor is assumed to decay with distance, with all sensors having identical sensing areas. They formulate the target detection problem as an unauthorized traversal problem and propose deployment strategies for minimizing the cost of the network that achieves the desired target detection probability. The authors proposed a deployment strategy where only part of the available sensors are randomly deployed. If the partial deployment satisfies the performance metric, no more sensors are deployed. Otherwise the process is repeated until the performance threshold is met.

In [11], the authors address the problem of optimum k-coverage of the boundary of an FoI. Covering the boundary of an FoI guarantees that any intruder will be detected with certainty. They assume that all sensors have identical sensing areas following the unit disk model as well. While target detection is guaranteed when the boundary of the FoI is covered, placement at the perimeter of the FoI does not yield the maximum target detection probability, when the boundary is not covered.

In [8], the authors address the problem of determining the delay until a target (intruder) is first detected. They consider the detection problem under the additional constraint that any sensor detecting the target must have a connected path to the sink. They assume that targets move in a straight line, and all sensors have identical sensing areas conforming to the unit disk model.

A relevant problem to target detection is the problem of target tracking. Once the target X has been detected, the WSN is used to track the motion of X within the FoI. Several methods for tracking moving targets with WSNs have been proposed in the literature [1], [10], [13], [17]. We do not address the problem of target tracking in this article.

III. Network Model Assumptions and Problem Mapping

A. Network Model Assumptions

Sensor Deployment and FoI: We assume that N sensors are deterministically placed within a planar FoI, $\mathcal{A}_0$. The FoI is assumed to be a connected and bounded set of perimeter L_0 of arbitrary shape. In case the FoI does not have a convex shape, the perimeter of the convex hull L_0^h is assumed to be known.

Target Model: We assume that mobile targets move on straight line trajectories, and all possible trajectories crossing the FoI appear with equal probability. Straight line trajectories minimize the length of the path for which a target remains exposed for detection. Hence, given an entry and exit point, the probability of detecting a target moving on a straight line yields the worst case probability compared to the detection of any other possible trajectory. The worst

TABLE I

THE MAPPING OF THE MOBILE TARGET DETECTION PROBLEM TO THE LINE-SET INTERSECTION PROBLEM

Mobile Target Detection	$\leftrightarrow$	**Line-Set Intersection**
Number of sensors N	$\leftrightarrow$	Number of sets N
Field of Interest $\mathcal{A}_0$	$\leftrightarrow$	Set S_0
Sensing area $\mathcal{A}_i$ of perimeter L_i	$\leftrightarrow$	Set S_i of perimeter L_i
WSN constellation	$\leftrightarrow$	Set constellation
Trajectory of target X	$\leftrightarrow$	Random line ℓ crossing S_0
Probability of detecting the target by at least one sensor: P_D	$\leftrightarrow$	*Probability of $\ell(\xi,\theta)$ intersecting at least one set*

case analysis allows us to provide probabilistic guarantees for the detection performance of the WSN. Straight line motion models have also been assumed in previous works addressing the target detection problem [4], [8], [10].

Sensing Model: We assume that each sensor $s_i, i = 1 \dots N$ has a sensing area A_i that is a closed and connected set of perimeter $L_i \ll L_0$. In the case where the sensing area is non-convex, we assume that the perimeter, denoted as L_i^h of the convex hull of A_i is known. Based on our assumptions, sensors need not have an identical sensing area A_i. For detecting a mobile target X we assume the Boolean detection model, where a target X is detected by a sensor s_i if the trajectory of X crosses the sensing area of s_i. The Boolean detection model has also been assumed in [4], [11].

B. Mapping the target detection problem to the line-set intersection problem

In this section we present the mapping of the target detection problem to the line-set intersection problem. This problem formulation provides the necessary tools to derive analytic formulas for the probability of target detection.

Target Detection Problem: *Given an FoI $\mathcal{A}_0$ of perimeter L_0, and N sensors with sensor s_i having a sensing area $\mathcal{A}_i$ of perimeter L_i, find the WSN constellation that maximizes the probability P_D of detecting a target X randomly crossing $\mathcal{A}_0$.*

Let the FoI be mapped to a bounded set S_0, defined as a collection of points in the plane. Let also the sensing area of sensor s_i be mapped to a bounded set S_i and the trajectory of the target X be mapped to a straight line $\ell(\xi,\theta)$ in the plane, with parameters ξ and θ be the shortest distance of ℓ to the origin, and θ be the angle of the normal to the line, with reference to the coordinate system, respectively. Then, the target detection problem is equivalent to the following line-set intersection problem, arising in Integral Geometry [15], [16].

Line-set Intersection Problem: *Given a bounded set S_0 of perimeter L_0, and N sets S_i of perimeter L_i, find the positions of S_i inside S_0 that maximize the probability P_D that a random line ℓ intersecting S_0, also intersects any of the N sets $S_i, i = 1 \dots N$.*

Table I summarizes the mapping from the mobile target detection problem to the line-set intersection problem. Throughout the rest of the paper $\mathcal{A}_i$ and S_i will be used interchangeably.

IV. SENSOR PLACEMENT FOR MAXIMIZING THE TARGET DETECTION PROBABILITY

In this section, we compute the target detection probability P_D as a function of the network parameters. First, we derive analytical formulas when only one sensor is deployed within the FoI. Then, we extend to the case where two sensors are deployed within the FoI, and show the placement of those sensors that maximizes P_D. We then generalize for the case of N sensors, and derive relevant lower and upper bounds on P_D, using the cases of one and two sensors as building blocks.

A. Probability of Detection by a Single Sensor

Assume that a single sensor $\mathcal{A}$ has been deployed within the FoI, $\mathcal{A}_0$. The probability P_D of detecting a target X crossing the FoI can be derived using a frequency count argument. The P_D can be computed as the quotient of the "number" of lines in the plane intersecting $\mathcal{A}_0$, over the "number" of lines intersecting both $\mathcal{A}_0, \mathcal{A}$. Since the set of lines in the plane intersecting a set $\mathcal{A}$ is uncountable, we use a measure defined in Integral Geometry [12], [15], [16].

Definition 1: **Measure of set of lines $m(\ell)$:** The measure $m(\ell)$ of a set of lines $\ell(\xi,\theta)$ is defined as the integral over the line density $d\ell = d\xi \wedge d\theta$, $m(\ell) = \int d\xi \wedge d\theta$, where $\wedge$ denotes the exterior product used in exterior calculus.

In the case where $\mathcal{A}$ is convex, the measure of the set of lines that intersect $\mathcal{A}$ is equal to:

$$m(\ell : \ell \bigcap \mathcal{A} \neq \emptyset) = \int_{\ell \bigcap \mathcal{A} \neq \emptyset} d\xi \wedge d\theta = \int_0^{2\pi} \xi d\theta = L, \quad (1)$$

where L is the perimeter of $\mathcal{A}$. Interested reader is referred to [15], for the proof of (1). In the case where $\mathcal{A}$ is non-convex, any line intersecting the convex hull of $\mathcal{A}$, also intersects $\mathcal{A}$. Hence, $m(\ell)$ is equal to the perimeter of the convex hull of $\mathcal{A}$. Once we have defined a measure for the set of lines intersecting a set $\mathcal{A}$, the probability of target detection by a single sensor, is given by the following theorem.

Theorem 1: The probability that a target X is detected by a sensor s with sensing area $\mathcal{A}$ of perimeter L, deployed within a FoI $\mathcal{A}_0$ of perimeter L_0 is given by

$$P_D = \frac{L}{L_0}. \quad (2)$$

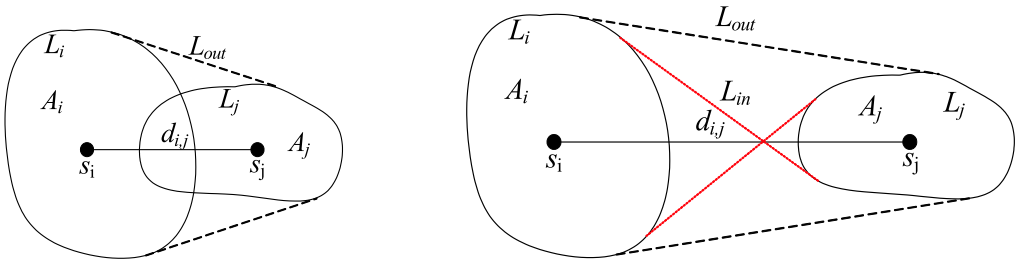

Fig. 2. The measure $m_2(d_{i,j})$ of the set of lines intersecting any of the two sensors is equal to (a) $L_{out}(d_{i,j})$ when $\mathcal{A}_i \cap \mathcal{A}_j \neq \emptyset$, (b) $L_i + L_j - (L_{in}(d_{i,j}) - L_{out}(d_{i,j}))$ when $\mathcal{A}_i \cap \mathcal{A}_j = \emptyset$.

Proof: The proof follows by noting that the probability of detecting a target is equal to the quotient of the measure of the set of lines intersecting both sets $\mathcal{A}_0, \mathcal{A}$, over the measure of the set of lines intersecting $\mathcal{A}_0$.

$$P_D = \frac{m(\ell : \ell \bigcap \mathcal{A} \bigcap \mathcal{A}_0 \neq \emptyset)}{m(\ell : \ell \bigcap \mathcal{A}_0 \neq \emptyset)} \overset{\text{(i)}}{=} \frac{m(\ell : \ell \bigcap \mathcal{A} \neq \emptyset)}{m(\ell : \ell \bigcap \mathcal{A}_0 \neq \emptyset)} \overset{\text{(ii)}}{=} \frac{L}{L_0}. \quad (3)$$

Step (i) is due to the fact that any line intersecting $\mathcal{A}$, also intersects $\mathcal{A}_0$ ($\mathcal{A} \subseteq \mathcal{A}_0$). Hence, the measure of the set of lines intersecting $\mathcal{A} \bigcap \mathcal{A}_0$ is equal to the measure of the set of lines intersecting $\mathcal{A}$. Step (ii) follows from (1). ■

Note that P_D is independent of the shape of $\mathcal{A}, \mathcal{A}_0$, but only depends on the perimeter of the sensing area and the FoI. Thus, sensors that have sensing areas of different shape but same perimeter, yield the same target detection probability. Also P_D has the same value, regardless of the position of $\mathcal{A}$ within $\mathcal{A}_0$, due to the fact that all possible trajectories (lines) of target X are considered equiprobable.

B. Probability of Detection by Two Sensors

Assume now that two sensors s_i, s_j can be placed anywhere within the FoI. The placement of the sensors that maximizes P_D is provided by the following theorem.

Theorem 2: The target detection probability P_D by two sensors s_i, s_j is maximized when s_i, s_j are placed at the opposite ends of the diameter[1] of the FoI, and is given by:

$$P_D = \frac{L_i + L_j - m_2(d_{i,j})}{L_0}, \quad (4)$$

with

$$m_2(d_{i,j}) = \begin{cases} L_i + L_j - L_{out}(d_{i,j}), & \mathcal{A}_i \bigcap \mathcal{A}_j \neq \emptyset \\ L_{in}(d_{i,j}) - L_{out}(d_{i,j}), & \mathcal{A}_i \bigcap \mathcal{A}_j = \emptyset, \end{cases} \quad (5)$$

where $d_{i,j}$ denotes the distance between s_i, s_j, $m_2(d_{i,j})$ denotes the measure of the set of lines intersecting *both* $\mathcal{A}_i, \mathcal{A}_j$, $L_{in}(d_{i,j})$ denotes the length of the inner string wrapped around $\mathcal{A}_i, \mathcal{A}_j$ as shown in figure 2(b), and $L_{out}(d_{i,j})$ denotes the length of the outer string wrapped around $\mathcal{A}_i, \mathcal{A}_j$ as shown in figures 2(a), 2(b).

[1]The diameter of the FoI is defined as the longest pairwise distance between two points within the FoI.

Proof: For the case of two sensors s_i, s_j, a mobile target X is detected if its trajectory crosses the sensing area of either s_i or s_j. Using the equivalence to the line-set intersection problem, the target detection probability P_D is the probability that a random line intersects any of the two sets $\mathcal{A}_i$, $\mathcal{A}_j$ placed within the FoI. Expressed in probability terms,

$$P_D = P(\ell \cap \mathcal{A}_i) + P(\ell \cap \mathcal{A}_j) - P(\ell \cap \mathcal{A}_i \cap \mathcal{A}_j) \overset{(i)}{=} \frac{L_i + L_j - m_2(d_{i,j})}{L_0}. \quad (6)$$

In Step (i), $P(\ell \cap \mathcal{A}_i), P(\ell \cap \mathcal{A}_j)$ are computed using Theorem 1, and are independent of the positions of the two sets $\mathcal{A}_i$ $\mathcal{A}_j$. However, the measure $m_2(d_{i,j})$ of the set of lines intersecting both $\mathcal{A}_i$ $\mathcal{A}_j$, is a function of the relative distance $d_{i,j}$ between $\mathcal{A}_i$ $\mathcal{A}_j$, and is computed based on the following two cases.

Case I – $\mathcal{A}_i \cap \mathcal{A}_j \neq \emptyset$: When the sensing areas $\mathcal{A}_i$, $\mathcal{A}_j$ overlap, as shown in figure 2(a), $\mathcal{A}_i$, $\mathcal{A}_j$ form a connected and bounded set $\mathcal{A}_c = \mathcal{A}_i \cup \mathcal{A}_j$, and the target X is detected if it crosses $\mathcal{A}_c$. According to (1), the measure of the set of lines intersecting the bounded and connected set $\mathcal{A}_c$ is equal to the perimeter of $\mathcal{A}_c$, when $\mathcal{A}_c$ is convex, or the perimeter of the convex hull of $\mathcal{A}_c$ when $\mathcal{A}_c$ is not convex (when $\mathcal{A}_c$ is convex, $\mathcal{A}_c$ is the convex hull of itself by definition).

For two sets intersecting, the convex hull can be found by wrapping a string around the two sets, as shown in figure 2(a). Any line intersecting with the convex hull of $\mathcal{A}_c$, is guaranteed to intersect with at least one of $\mathcal{A}_i$, $\mathcal{A}_j$. Using Theorem 1, the target detection probability by two sensors with intersecting sensing areas is equal to:

$$P_D = \frac{L_i + L_j - m_2(d_{i,j})}{L_0} = \frac{L_{out}(d_{i,j})}{L_0}, \quad \mathcal{A}_i \bigcap \mathcal{A}_j \neq \emptyset, \quad (7)$$

where $L_{out}(d_{i,j})$ denotes the length of the perimeter of the convex hull of $\mathcal{A}_c$ (outer string in figure 2(a)). From (7), the measure of the set of lines intersecting both $\mathcal{A}_i$, $\mathcal{A}_j$ is, $m_2(d_{i,j}) = L_i + L_j - L_{out}(d_{i,j})$.

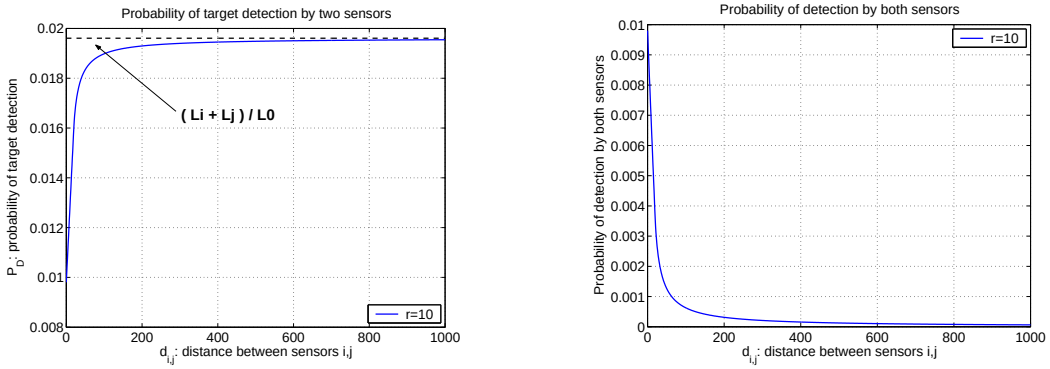

(a) (b)

Fig. 3. The target detection probability P_D achieved by two sensors, as a function of the pairwise distance $d_{i,j}$ between the sensors, when each sensors has a circular sensing area of radius $10m$. P_D is a monotonically increasing function of $d_{i,j}$ that asymptotically approaches $\frac{L_1+L_2}{L_0}$. (b) The probability that a target is detected by *both* sensors is a monotonically decreasing function of the pairwise distance $d_{i,j}$, asymptotically approaching zero.

Case II – $\mathcal{A}_i \cap \mathcal{A}_j = \emptyset$: When the sensing areas $\mathcal{A}_i,\ \mathcal{A}_j$ do not overlap, as shown in figure 2(b), $\mathcal{A}_i,\ \mathcal{A}_j$ no longer form a connected and bounded set. Sylvester showed that the measure of all lines that intersect both $\mathcal{A}_i,\ \mathcal{A}_j$ is equal to $m_2(d_{i,j}) = L_{in}(d_{i,j}) - L_{out}(d_{i,j})$ [16]. Hence in the case of non-overlapping $\mathcal{A}_i,\ \mathcal{A}_j$, P_D is equal to:

$$\begin{aligned} P_D &= \frac{L_i + L_j - m_2(d_{i,j})}{L_0} \\ &= \frac{L_i + L_j - (L_{in}(d_{i,j}) - L_{out}(d_{i,j}))}{L_0}. \end{aligned} \quad (8)$$

Note that as $d_{i,j} \to \infty$, $(L_{in}(d_{i,j}) - L_{out}(d_{i,j})) \to 0$, regardless of the shape and size of $\mathcal{A}_i, \mathcal{A}_j$, since the inner and outer string placed around the sensing areas become asymptotically equal in length. That is, $m_2(d_{i,j})$ *is a monotonically decreasing function of the pairwise distance* $d_{i,j}$,

$$\begin{aligned} \lim_{d\to\infty} P_D &= \lim_{d\to\infty} \frac{L_i + L_j - m_2(d_{i,j})}{L_0} \\ &= \frac{L_i + L_j}{L_0} - \frac{1}{L_0} \lim_{d\to\infty} (L_{in}(d_{i,j}) - L_{out}(d_{i,j})) \\ &= \frac{L_i + L_j}{L_0}. \end{aligned} \quad (9)$$

In figure 3(a), we show the asymptotic behavior of P_D, as a function of $d_{i,j}$, for the case of two sensors. We observe that as $d_{i,j}$ increases, P_D tends to the asymptotic value of $\frac{L_i+L_j}{L_0}$. In figure 3(b), we show the monotonically decreasing behavior of the probability that a target crosses both sensing areas. As $d_{i,j} \to \infty$, $\frac{m_2(d_{i,j})}{L_0} \to 0$.

Based on (9), the target detection probability P_D increases when the distance $d_{i,j}$ among $\mathcal{A}_i,\ \mathcal{A}_j$ increases. Given the boundary of the FoI, P_D is maximized when $d_{i,j}$ is maximized, which occurs when $\mathcal{A}_i,\ \mathcal{A}_j$ are placed at the opposite ends of the diameter of the FoI. In figure 4, we show the optimal placement of two sensors in the diameter of an FoI. ■

In the general case where $\mathcal{A}_i,\ \mathcal{A}_j$, have an arbitrary shape, an analytic formula for L_{in}, L_{out} may not be obtainable. Instead, $L_{in}(d_{i,j}), L_{out}(d_{i,j})$ may be measured, given that

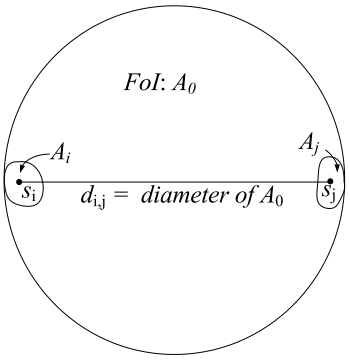

Fig. 4. Optimal placement of two sensors that maximizes the target detection probability P_D. Sensors s_i, s_j are placed at the opposite ends of the diameter of the FoI.

$\mathcal{A}_i,\ \mathcal{A}_j$ are known. On the other hand, for specific shapes of $\mathcal{A}_i,\ \mathcal{A}_j$, the lengths L_{in}, L_{out} can be expressed as a function of the distance $d_{i,j}$ among the shapes. As an example, for two circles with radius r,

$$\begin{aligned} L_{out} &= 2(\pi r + d_{i,j}), \\ L_{in} &= 2\pi r + 2d_{i,j}\sqrt{1 - \left(\frac{2r}{d_{i,j}}\right)} + 4\sin^{-1}\left(\frac{2r}{d_{i,j}}\right), \end{aligned}$$

when $d_{i,j} \geq 2r$. In the next section we utilize the P_D formula for the case of two sensors, in order to derive a lower bound on P_D for the case of N sensors.

C. Generalization to the Probability of Detection by N Sensors

When N sensors can be placed within the FoI, the probability of detecting a moving target is expressed based on the inclusion-exclusion principle for unions of sets [9], [16].

Theorem 3: Let a target X cross an FoI of perimeter L_0. Let N sensors be placed within the FoI at any desired position. The probability of detection P_D is given by:

$$\begin{aligned} P_D &= \sum_{i=1}^{N} P(\ell \cap \mathcal{A}_i \neq \emptyset) - \sum_{i,j,\ i<j} P(\ell \cap \mathcal{A}_i \cap \mathcal{A}_j \neq \emptyset) \\ &\quad + \ldots + (-1)^{N+1} P(\ell \cap \mathcal{A}_1 \cap \ldots \cap \mathcal{A}_N \neq \emptyset). \end{aligned} \quad (10)$$

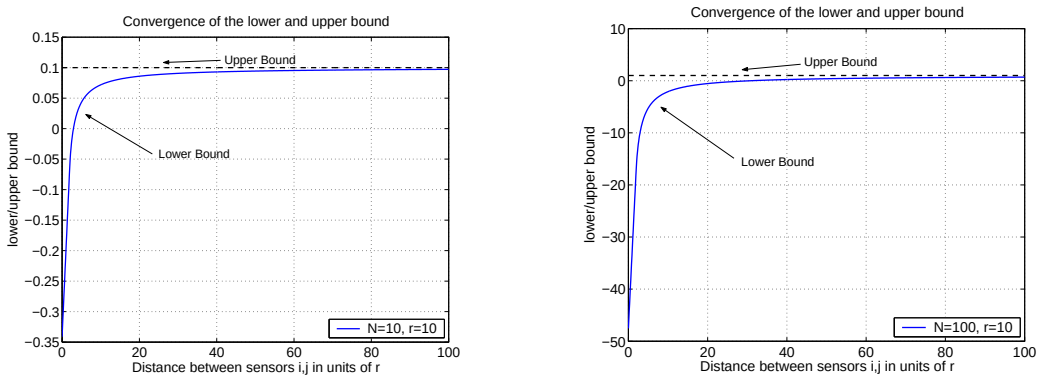

(a) (b)

Fig. 5. Convergence of the lower bound of P_D to the upper bound of P_D with the increase of the pairwise distance $d_{i,j}$ for a WSN of (a) 10 nodes, (b) 100 nodes. The x-axis denotes the pairwise distance normalized in units of the sensing range of the sensors r.

Proof: Given that N sensors are placed within the FoI, the probability that target X is detected is equivalent to the probability that X crosses the sensing area of at least one sensor. Expressing this statement in terms of probability events, we have

$$P_D = P(\ell \cap \mathcal{A}_1 \cup \mathcal{A}_2 \cup \ldots \cup \mathcal{A}_N). \tag{11}$$

By applying the inclusion-exclusion principle [9], P_D is expressed using the sum of conjunctive probabilities of a line intersecting specific arrangements of sets.

$$\begin{aligned} P_D &= P(\ell \cap \mathcal{A}_1 \neq \emptyset) + P(\ell \cap \mathcal{A}_2 \neq \emptyset) \ldots \\ &+ P(\ell \cap \mathcal{A}_N \neq \emptyset) - P(\ell \cap \mathcal{A}_1 \cap \mathcal{A}_2 \neq \emptyset) \\ &\quad -P(\ell \cap \mathcal{A}_1 \cap \mathcal{A}_N \neq \emptyset) \ldots \\ &\quad +(-1)^{N+1} P(\ell \cap \mathcal{A}_1 \cap \mathcal{A}_2 \ldots \cap \mathcal{A}_N \neq \emptyset) \\ &= \sum_{i=1}^{N} P(\ell \cap \mathcal{A}_i \neq \emptyset) - \sum_{i,j,\ i<j} P(\ell \cap \mathcal{A}_i \cap \mathcal{A}_j \neq \emptyset) \\ &\quad + \ldots + (-1)^{N+1} P(\ell \cap \mathcal{A}_1 \cap \mathcal{A}_2 \ldots \cap \mathcal{A}_N \neq \emptyset). \end{aligned}$$

■

While Theorem 3 expresses the exact analytic formula for P_D, the number of terms in (10) is $(2^N - 1)$. Furthermore, for arbitrary set arrangements, analytic expressions of the probability of a line intersecting exactly k sets are not known, except for small values of k [16]. Hence, we consider the following lower and upper bounds for finite unions.

Corollary 1: The probability of target detection P_D is bounded by:

$$\begin{aligned} LB &\leq P_D < UB, \qquad (12) \\ LB &= \sum_{i=1}^{N} P(\ell \cap \mathcal{A}_i \neq \emptyset) - \sum_{i,j,i<j} P(\ell \cap \mathcal{A}_i \cap \mathcal{A}_j \neq \emptyset), \\ UB &= \sum_{i=1}^{N} P(\ell \cap \mathcal{A}_i \neq \emptyset). \end{aligned}$$

Proof: This is a special case of the Bonferroni inequalities [9]. ■

Both the lower and upper bound in (13), can be evaluated using the results of Theorems 1, 2:

$$\begin{aligned} LB &\leq P_D < UB, \qquad (13) \\ LB &= \frac{1}{L_0}\left(\sum_{i=1}^{N} L_i - \sum_{i,j,\ i<j} m_2(d_{i,j})\right), \qquad (14) \\ UB &= \frac{1}{L_0}\sum_{i=1}^{N} L_i. \qquad (15) \end{aligned}$$

The lower bound in (15) is exact for sensor constellations where no lines intersect more than two sensors. However, we note that P_D can never achieve the upper bound for $N > 1$ since there will always be a non-zero number of lines crossing two sensing areas. The lower bound approaches the upper bound as the pairwise distances $d_{i,j}$ among each pair of sensors increase. This is a consequence of the asymptotic behavior of P_D for $N = 2$, as we showed in section IV-B. Hence, by increasing the pairwise distance $d_{i,j}$ among each pair of sensors, the lower bound of P_D tends to the upper bound and, hence, P_D attains its maximum value,

$$\begin{aligned} \lim_{d_{i,j}\to\infty} LB &= \frac{1}{L_0}\left(\sum_{i=1}^{N} L_i - \sum_{i,j,\ i<j} m_2(d_{i,j})\right) \\ &= \frac{1}{L_0}\sum_{i=1}^{N} L_i - \frac{1}{L_0}\sum_{i,j,\ i<j} \lim_{d_{i,j}\to\infty} m_2(d_{i,j}) \\ &= \frac{1}{L_0}\sum_{i=1}^{N} L_i. \qquad (16) \end{aligned}$$

In figure 5(a), we show the values for the lower and upper bound of P_D as a function of the pairwise distance among sensors. The sensing areas of the sensors are assumed disks with radius $r = 10m$ while the FoI is assumed to be a disk of radius $R = 1000m$. The x axis is normalized to the radius of the sensing areas of the sensors. We observe that for small values of the pairwise distance, the lower bound does not reflect the actual value of P_D. In fact, the lower bound has negative value since the higher order terms that are ignored (probabilities that lines cross three or more sensing areas)

TABLE II

ANALOGY OF THE TARGET DETECTION PROBABILITY TO THE SYMBOL ERROR PROBABILITY

Mobile Target Detection	$\leftrightarrow$	**Symbol Error over AWGN**
Number of sensors N	$\leftrightarrow$	Number of symbols N
Field of Interest $\mathcal{A}_0$	$\leftrightarrow$	Maximum symbol energy
Sensor constellation	$\leftrightarrow$	Symbol constellation
Pairwise distance $d_{i,j}$ among sensors	$\leftrightarrow$	Pairwise distance $d_{i,j}$ among symbols
Monotonically decreasing function $m_2(d_{i,j})$	$\leftrightarrow$	Monotonically decreasing function $P(b_i \rightarrow b_j)$
Maximize the probability of target detection	$\leftrightarrow$	*Minimize the symbol error probability*

are significant. However, when the pairwise distances become sufficiently large, $(d_{i,j} \geq 20r)$, the lower bound approaches the upper bound and P_D tends asymptotically to the upper bound. Similarly, in figure 5(b), we show the convergence of the lower and upper bound for $N = 100$ sensors. For larger N the lower and upper bound converge slower compared to the case of $N = 10$.

V. ANALOGY OF TARGET DETECTION TO DIGITAL MODULATION SCHEMES

Maximizing the lower bound in (15), provides a worst case probabilistic guarantee on target detection. The first sum of the lower bound in (15) is independent of the sensors' positions. On the other hand, the sum $\sum_{i,\ i<j} m_2(d_{i,j})$ is a function of the pairwise distance $d_{i,j}$. In Section IV-B, we showed that $m_2(d_{i,j})$ is a positive monotonically decreasing function of $d_{i,j}$. Hence, increasing $d_{i,j}$ also increases the lower bound in (15). In fact, for sensor constellations where no lines intersect more than two sets, the lower bound is exact and hence, increasing the lower bound also increases P_D.

The problem of finding the sensor constellation that maximizes the lower bound in (15) is analogous to the problem of finding a 2-dimensional signal constellation that minimizes the average probability of symbol error P_{SE}, over an AWGN channel. Assuming that all symbols are equiprobable, P_{SE} is expressed as a function of the pairwise error probability $P(b_i \rightarrow b_j)$ between two symbols b_i, b_j. $P(b_i \rightarrow b_j)$ is a monotonically decreasing function of $d_{i,j}$ between the two symbols [2]. For a constellation with N equiprobable symbols, P_{SE} is upper bounded by,

$$\begin{aligned} P_{SE} &\leq \frac{1}{N} \sum_{i,i<j} P(b_i \rightarrow b_j) \\ &= \frac{1}{N} \sum_{i,i<j} \frac{1}{2} \text{erfc}\left(\frac{d_{i,j}}{2\sqrt{N_0}}\right), \end{aligned} \tag{17}$$

where erfc denotes the error function, and $\frac{N_0}{2}$ denotes the power spectral density of the channel noise component. Both the problem of maximizing the lower bound in (15) and the analogous problem of minimizing P_{SE}, require the minimization of a multivariate function which is a summation of identical functions, monotonically decreasing with respect to each variable. This problem analogy is presented in Table II.

In digital communications, the minimum pairwise distance among symbols is the dominant factor of symbol error, due to the exponential decrease of $P(b_i \rightarrow b_j)$ with $d_{i,j}$ [2]. Hence, good symbol constellations maximize the minimum pairwise distance among symbols. Due to the analogy presented in Table II, we consider solutions that maximize the minimum pairwise distance for the target detection problem. The problem of maximizing the minimum pairwise distance among points in the plane, can be addressed using as an intermediate step the following circle packing problem [7]. *Given N circles $C_i,\ i = 1 \ldots N$, compute the maximum radius of the circles that would fit inside a given planar set $\mathcal{A}_0$.*

The circle packing problem (sphere packing in 3-dimensions), has known optimal solutions for small values of N, and certain shapes of FoI, such as circle, square, hexagonal or triangle, but no optimal solutions exist for large N [2], [3]. However, good signal constellations can be carved from lattices with high circle packing density [7]. In figure 6(a), we show the optimum placement of circles that maximize the minimum pairwise distance among the circles, for a circular FoI, for $N = 2 \ldots 9$. In figure 6(b), we show the optimum placement for the case of a square FoI.

Note that the circles C_i defined from the circle packing problem do not correspond to the sensing areas $\mathcal{A}_i$ of the sensors. Instead they provide the area C_i where each sensor s_i should be placed. Assuming that $\mathcal{A}_i \ll C_i$ which holds true when $\mathcal{A}_i \ll \mathcal{A}_0$ and N is not sufficient to cover the FoI, the position of the sensors within C_i, is chosen so that the sensing areas have maximum pairwise distance. As an example, in figure 6(a) for the case of $N = 2$, the sensors are placed within C_1, C_2 so that the sensing areas have maximum $d_{i,j}$. For networks with heterogeneous sensing areas, sensors are placed within each C_i with the s_i with larger L_i be placed further apart.

VI. PERFORMANCE EVALUATION

In this section we evaluate the performance of our heuristics with respect to other sensor placement solutions such as random deployment. We also illustrate the impact of network parameters such as length of perimeters of sensing areas.

A. Methodology

We first deployed N sensor nodes within the FoI according to a predefined algorithm such as one of our heuristics or randomly. For each network instance, we generated 10,000 random target trajectories and measured the fraction of trajectories that intersect with the sensing area of one or more sensors. For deterministic deployments one trial was sufficient to statistically estimate the target detection probability, since the placement of the sensors does not change over trials and

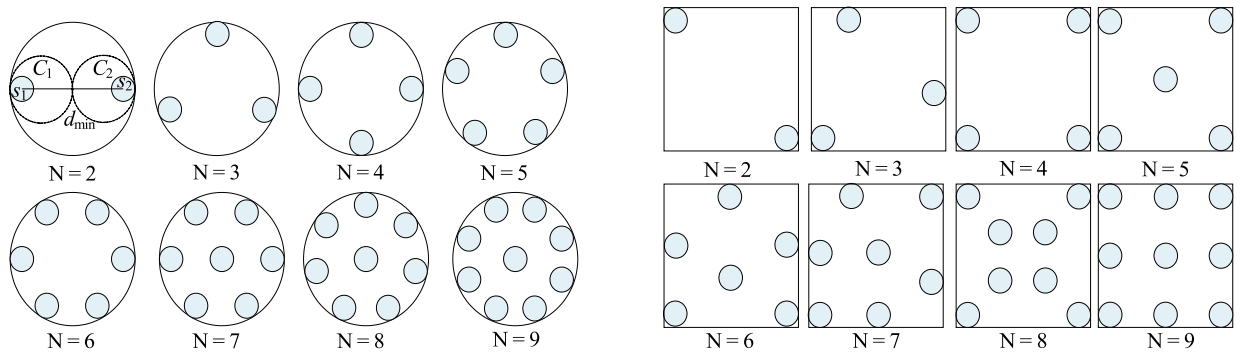

Fig. 6. The sensor constellations that maximize the minimum pairwise distance among sensors for, (a) a circular FoI, (b) a square FoI. The shaded circles denote the sensing area of each sensor.

sufficient number of trajectories are considered to guarantee statistical validity. For random deployments, we repeated the experiment for 100 network deployments in order to compute the average target detection probability.

We initially considered homogeneous WSN where all nodes had identical sensing areas. The experiments for the homogeneous case provide an easy interpretation of the behavior of P_D with respect to network parameters. We then performed our experiments in heterogeneous WSN. To simulate heterogeneous WSN, we generated a pool of sensing areas of different shapes (circle, square, triangle, pentagon, hexagon) and varying lengths, and randomly selected N to be placed within the FoI.

B. Target Detection Probability for Homogeneous WSN

In our first experiment, we placed $N = 2 \ldots 9$ sensors in a circular FoI of radius $R = 100m$, according to the WSN constellations shown in figure 6(a). Sensors had identical sensing ranges that varied from $r = 5m$ to $r = 20m$. We measured the target detection probability P_D and also computed the analytical lower bound given by (15). In figure 7(a), we show the target detection probability P_D vs. the number of sensors deployed for varying r and the corresponding lower bound.

We observe that for small values of r ($r = 5m,\ 10m$) the lower bound provides a very good estimate of the actual value of P_D. This is due to the fact that no lines intersect more than two sensing areas. Hence, the lower bound in (15) that takes into account only lines that intersect one or two sensing areas is exact. Furthermore, we observe that for small values of r the P_D increases almost linearly with the number of sensors deployed. This is due to the fact that the measure $m_2(d_{i,j})$ of lines that intersect two sensing areas is very small when the pairwise distance among the sensors is sufficiently large compared to their sensing range. This is illustrated in figure 2(b) where we show that when $d_{i,j} = 20r$ the probability that a line intersects two sensing areas is almost negligible. Hence, for these values of r, the lower bound approaches the upper bound and P_D is maximized.

For larger values of sensing range r and WSN values of $N \geq 6$ we observe that the lower bound starts to deviate from the probability of detection P_D. In fact, the lower bound starts to decrease with the increase of N. This is due to the fact that for large values of r and N, the probability that a line would intersect three or more sensing areas is non-negligible and hence, omitting this additive factor from the lower bounds yields its deviation from the true value of P_D.

In figure 7(b), we show the target detection probability P_D for the WSN constellations shown in figure 6(b). The FoI is now a square with each side being $\alpha = 100m$. Again we observe that for small values of r the lower bound is very tight to the value of P_D obtained via the simulation, while the lower bound deviates from P_D for large values of r, N.

In our second experiment, we compared the target detection probability achieved by our heuristic with the target detection probability achieved by random sensor deployment. Although this comparison is unfair since random deployments yield lower performance due to overlapping sensing areas, it is an indicator of the performance gains that can be achieved by adopting a deterministic solution. For each value of N we randomly deployed the N sensors within the FoI and measured P_D. We repeated the same experiment 100 times and averaged the result. In figure 8(a), we show the target detection probability for $N = 2 \ldots 40$ and for a sensing range $r = 5m$. We observe the our placement algorithm yields a performance gain up to 14% compared to random deployment (average case), while random deployment can yield WSN constellations that are up to 90% worse.

In figure 8(b), we show P_D for $N = 2 \ldots 14$ and for a sensing range $r = 20m$. For $r = 20m$ we considered WSN of smaller sizes since larger WSN would be able to entirely cover the boundary of the FoI thus yielding a $P_D = 1$. We observe that for sensing areas of larger perimeter, the gains are even greater, due to the higher sensing area overlap in random deployments. Our heuristic yields a P_D up to 18% higher compared to the performance of the random deployment.

The benefits from adopting our placement strategy are even more significant, when the savings in number of sensors is considered. From figure 8(a), we observe that we requires26 sensors to achieve a target detection probability of $P_D = 0.8$. On the other hand, 40 sensors are required to achieve the same target detection probability using random deployment, that is, 54% more sensors are required in the random deployment case.

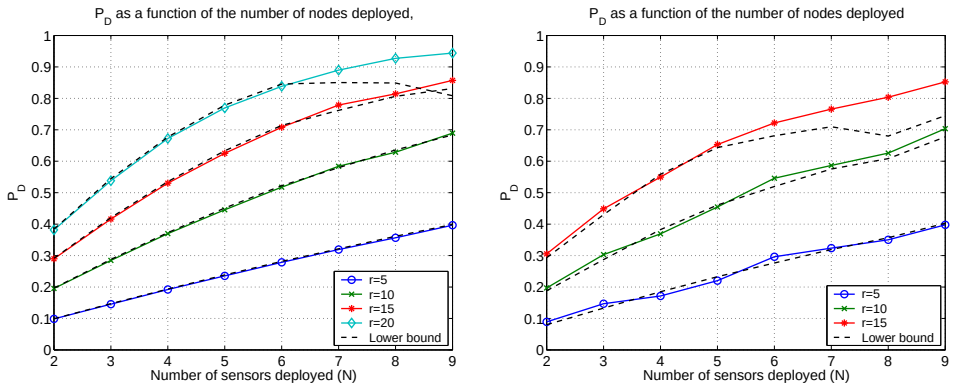

(a) (b)

Fig. 7. The target detection probability P_D as a function of the number of sensors deployed and the sensing range radius r for the sensor constellations of, (a) figure 6(a), (b) figure 6(b).

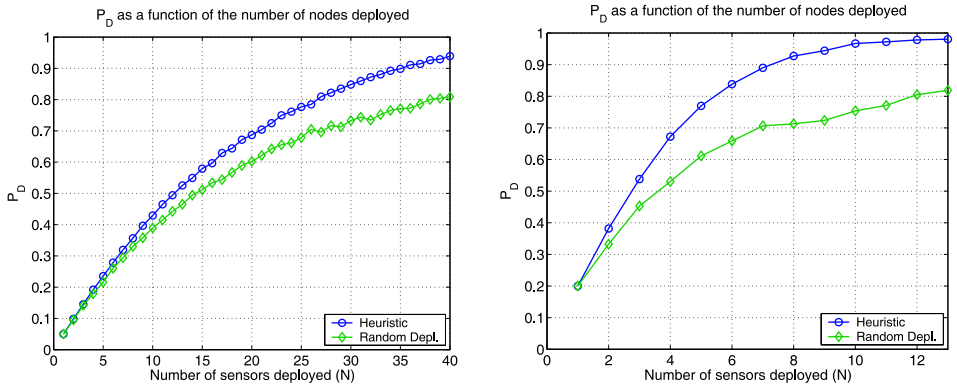

(a) (b)

Fig. 8. Comparison of the performance of our heuristic vs. random deployment for homogeneous WSN with sensing range (a) $r = 5m$, (b) $r = 20m$.

Similarly, from figure 8(b), we observe that we need to place only five sensors to achieve a target detection probability of $P_D = 0.78$. On the other hand, 11 sensors are required to achieve the same target detection probability using random deployment, that is, 120% more sensors are required in the random deployment case.

C. Target Detection Probability for Heterogeneous WSN

For the case of heterogeneous WSN, we repeated the experiments we conducted for the homogeneous case by placing nodes with heterogeneous sensing areas. The shape and size of the sensing areas were randomly selected from a pool of five shapes (circular, square, triangle, pentagon, hexagon). In figure 9, we show the target detection probability for WSN of different sizes and as a function of the sensing range r. For the heterogeneous WSN case, the sensing range denotes a circle where the sensing area of each sensor can be inscribed. As an example when the sensing area of the selected node is square, the side of the sensing area is equal to $\alpha = \sqrt{(2)}r$, and its perimeter equal to $L_i = 4\sqrt{(2)}r$.

We observe that in the heterogeneous case, the lower bound still accurately predicts the target probability of detection when the sensing range is small. For higher values of r the lower bound deviates from P_D indicating that a significant number of lines intersect with more than two sensing areas. Also, compared to the homogeneous case, the target detection probability does not exhibit a linear behavior. This is due to the fact that the perimeters of the sensing areas are no longer constant, but vary with the shape of the sensing areas.

We also repeated the comparison of our placement algorithm with a random sensor deployment strategy, for heterogeneous WSN. In figure 10, we show the target detection probability as a function of the WSN size. As expected, our placement algorithm performs better than the random deployment strategy, with the difference in performance increasing as the number of sensors deployed also increases. Regardless of the shapes of the sensing areas and the lengths of the perimeters, random deployment can result in overlapping sensing areas and sensors with constellations with small pairwise distances, thus having inferior performance to deterministic deployment.

VII. Conclusion

We addressed the problem of deterministic deployment of WSN for maximizing the target detection probability P_D. We derived analytic formulas expressing P_D, by mapping the target detection problem to the line-set intersection problem. Our formulation allowed the consideration of WSN with heterogeneous sensing capabilities. We showed that the analytic expressions of P_D are not practical for large N and derived lower and upper bounds. We finally showed that maximizing

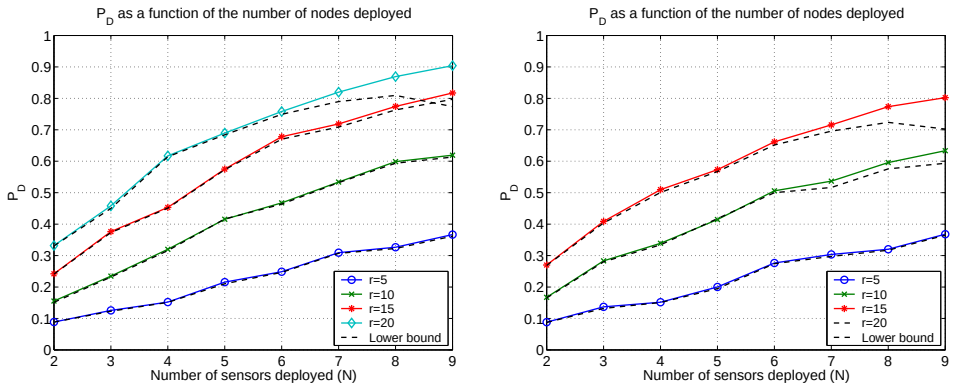

Fig. 9. The target detection probability P_D as a function of the number of sensors deployed and the sensing range radius r for the sensor constellations of, (a) figure 6(a), (b) figure 6(b). The sensors deployed have heterogeneous sensing capabilities.

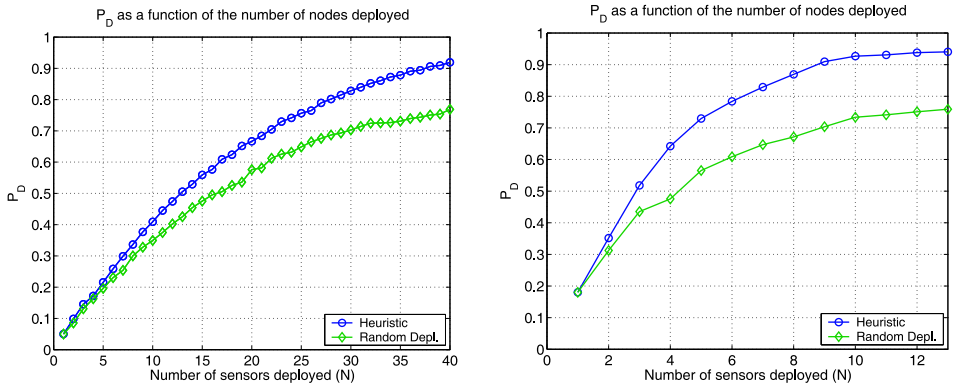

Fig. 10. Comparison of the performance of our heuristic vs. random deployment for heterogeneous WSN with sensing range (a) $r = 5m$, (b) $r = 20m$.

the lower bound, is analogous to minimizing the average symbol error probability in 2-dimensional modulation schemes, over an AWGN channel and derived WSN constellations from well known signal constellations.

ACKNOWLEDGEMENTS

This work was supported in part by the following grants: ONR YIP award, N00014-04-1-0479, ARO PECASE grant, W911NF-05-1-0491, and ARL CTA Grant DAAD 19-01-2-0011.

REFERENCES

[1] J. Aslam, Z. Butler, F. Constantin, V. Crespi, G. Cybenko, and D. Rus, "Tracking a Moving Object with a Binary Sensor Network," In Proc. of the 1st international Conference on Embedded Networked Sensor Systems, Nov. 2005, pp. 150-161.

[2] S. Benedetto, and E. Biglieri "Principles of Digital Transmission With Wireless Applications," NY, Kluwer, 1999.

[3] J. Boutros, E. Viterbo, C. Rastello, and J. Belfiore, "Good lattice constellations for both Rayleigh fading and Gaussian channels," *IEEE Transactions on Information Theory*, Vol. 42, No. 2, 1996, pp. 502-518.

[4] Q. Cao, T. Yan, T. Abdelzaher, and J. Stankovic, "Analysis of Target Detection Performance for Wireless Sensor Networks," In Proc. of the International Conference on Distributed Computing in Sensor Networks, CA, June 2005.

[5] K. Chakrabarty, S. Iyengar, H. Qi and E. Cho, "Grid Coverage for Surveillance and Target Location in Distributed Sensor Networks," IEEE Transactions on Computers, vol. 51, pp. 1448-1453, December 2002.

[6] T. Clouqueur, V. Phipatanasuphorn, P. Ramanathan, and K. K. Saluja, "Sensor Deployment Strategy for Target Detection", Proc. of the 1st ACM International Workshop on Wireless Sensor Networks and Applications, Sep. 2002, pp. 42–48.

[7] J. H. Conway, and N. J. Sloane, "Sphere Packings, Lattices and Groups," 3nd ed. NY Springer-Verlag, 1998.

[8] O. Dousse, C. Tavoularis, and P. Thiran, "Delay of Intrusion Detection in Wireless Sensor Networks," In Mobihoc 2006.

[9] W. Feller, *An Introduction to Probability Theory and its Applications*, 3rd edition, John Wiley and Sons Inc.

[10] C. Gui, and P. Mohapatra, "Power Conservation and Quality of Surveillance in Target Tracking Sensor Networks," In Proc. of the 10th Annual International Conference on Mobile Computing and Networking, Sept. 2004, pp. 129-143.

[11] S. Kumar, T.H. Lai, and A. Arora, "Barrier coverage with wireless sensors," in Proc. of the 11th Annual International Conference on Mobile Computing and Networking (MoBiCom '05), 2005, pp. 284–298.

[12] L. Lazos, R. Poovendran, and J. A. Ritcey, "Probabilistic Detection of Mobile Targets in Heterogeneous Sensor Networks," Technical Report, available at http://www.ee.washington.edu/research/nsl/papers/TRdetection06.pdf.

[13] D. Li, K. Wong Y.H. Hu, and AM Sayeed, "Detection, classification, and tracking of targets in distributed sensor networks," *Signal Processing Magazine*, IEEE, 2002, Vol. 19, No. 2, pp. 17–29.

[14] S. Meguerdichian, F. Koushanfar, G. Qu, and M. Potkonjak, "Exposure In Wireless Ad Hoc Sensor Networks," In Proc. of MOBICOM 2001, July 2001, pp. 139–150.

[15] L. Santalo, *Integral Geometry and Geometric Probability*, Addison-Wesley Publishing Company, 1976.

[16] J. Sylvester, "On a Funicular Solution of Buffon's Needle Problem," Acta. Math. 14, 1890, pp. 185-205.

[17] H. Yang, and B. Sikdar, "A protocol for tracking mobile targets using sensor networks," in Proc. of the First IEEE. 2003 International Workshop on Sensor Network Protocols and Applications, pp. 71–81.